Desalination and Water Treatment
www.deswater.com
doi: 10.5004/dwt.2021.27339

228 (2021) 297–311
July

Removal of heavy metal ions from aqueous solution by anionic polyacrylamide-based monolith: equilibrium, kinetic and thermodynamic studies

Ayat Allah Al-Massaedh[a,*], Fawwaz I. Khalili[b]

[a]*Department of Chemistry, Faculty of Science, Al al-Bayt University, 25113 Mafraq, Jordan, email: almassaedh@aabu.edu.jo*
[b]*Department of Chemistry, Faculty of Science, The University of Jordan, 11942 Amman, Jordan*

Received 10 January 2021; Accepted 15 April 2021

ABSTRACT

In the present study, a macroporous polyacrylamide-based monolith bearing negatively charged sulfonic acid groups was synthesized as a new adsorbent for the removal of heavy metals ions (Pb^{2+}, Cd^{2+}, and Cr^{3+}) from aqueous solutions. Vinylsulfonic acid was selected as an anionic monomer to introduce a negative charge on the surface of the resulting monolith that forms a complex with investigated metal ions. The influences of solution pH, contact time, monolith dosage, initial concentration, and temperature on Pb^{2+}, Cd^{2+}, and Cr^{3+} removal were determined using the batch equilibrium technique. Adsorption data were modeled with Langmuir, Freundlich, and Dubinin–Raduskevich isotherm models. The experimental equilibrium data for Pb^{2+}, Cd^{2+}, and Cr^{3+} using the synthesized monolith showed a good correlation with the Langmuir isotherm model. Based on the Langmuir model, the maximum monolayer adsorption capacities of the monolith were 22.8 mg g^{-1} for Cd^{2+}, 33.3 mg g^{-1} for Pb^{2+}, and 66.7 mg g^{-1} for Cr^{3+} at 25°C. Kinetic studies revealed that the adsorption of the metal ions onto the monolith followed pseudo-second-order kinetics. The negative and positive values of free energy ($\Delta G°$) and enthalpy ($\Delta H°$) revealed that the adsorption of the metal ions onto the monolith was spontaneous and endothermic, respectively.

Keywords: Heavy metals removal; Polyacrylamide monolith; Adsorption; Isotherms; Kinetics; Metal; Thermodynamics

1. Introduction

Pure water is an essential requirement for human, animal, and plant life [1–3]. It has a significant impact on human health, food, the environment, and the economy [4]. For a healthy life, water resources must be free of different types of pollutants that are detrimental to human or animal health. During the last years, contamination of water resources was dramatically raised due to rapid and unorganized industrial and urban developments. Water resources can be contaminated by several types of toxic contaminants organic, biological, or heavy metals due to different anthropogenic sources such as smelting, pesticides, industries, insecticides, automobile emissions, fertilizers, sewage sludge, and chemical industrial wastes (e.g., paints, batteries, textile, electroplating, or paper manufacturing) [3,5–8]. Heavy metals such as cobalt (Co), cadmium (Cd), lead (Pb), mercury (Hg), tin (Sn), nickel (Ni), or arsenic (As) are hazardous and carcinogenic environmental contaminants that are non-biodegradable, thermostable, and have long biological half-lives [2,9–11]. Therefore, they have a strong ability to accumulate to higher levels in different media such as surface water, soils, air, plants, and sediments, and consequently, causing a serious risk on human health [9,12,13].

Different conventional methods have been employed for the removal of toxic heavy metals from contaminated water resources such as chemical precipitation,

* Corresponding author.

coagulation/flocculation, ion exchange, chemical oxidation, electrodialysis, photocatalysis, and membrane filtration [2,3,5–7,11,14–17]. However, these methods show several drawbacks like low removal efficiency, consuming a large amount of chemicals, need high-energy requirements, low selectivity, high operational costs, long duration time, and generation of large volumes of disposal sludge and other toxic products [6,17,18]. An attractive alternative to these methods is the use of the adsorption method for water purification due to its high removal efficiency, easy handling, availability of a wide variety of adsorbents, ease to regenerate, and low cost [2,3,5,19–25]. In general, adsorption is a surface phenomenon including (i) a mass transfer of adsorbate molecules from the liquid phase to the adsorbent surface, (ii) adsorption of these molecules by forming physical or chemical interactions, (iii) diffusion of adsorbate molecules within the adsorbent particle [6,26]. In the literature, several factors have been reported to affect the adsorption process such as pH, ionic strength, temperature, type of adsorbate, type of adsorbent, the time needed for equilibrium, initial adsorbate concentration, and surface area and pore volume of adsorbent [2,3,20,24,25,27,28]. In this context, different types of adsorbents either synthetic or natural have been used for the removal of toxic pollutants from aqueous solutions including: activated carbon [7,25,27,29,30], metal oxide nanoparticles [11,20,31], functionalized silica gel [32], hydroxyapatite [33], chitosan [34], bentonite [35], zeolite [27,36,37], humic acid [38], silica-based and metal-oxide monoliths [39,40], organic-inorganic nanocomposite ion exchangers [23], and vegetable and fruit peels [8]. During the last years, macroporous organic-based monoliths have gained great interest as a unique material used in analytical and bioanalytical chemistry applications such as chromatography, extraction, catalyst supports, or purification [41–48]. This is due to their ease of production in various shapes and dimensions, high porosity, reproducibility of the synthesis procedures, high capacity, flexible framework, chemical stability, and availability of a wide variety of suitable monomers [29,43,49,50].

Uzun et al. [46] synthesized poly(hydroxyethyl methacrylate) monolith containing chelating cysteine functionality by copolymerization of hydroxyethyl methacrylate and *N*-methacryloyl-(L)-cysteine methyl ester in a glass tube. The formed monoliths were utilized for the removal of Cu^{2+}, Cd^{2+}, Zn^{2+}, Hg^{2+}, and Pb^{2+} ions from aqueous solutions. The authors found that the maximum adsorption capacities of the formed monolith were 68.2, 129.2, 245.8, 270.2, and 284.0 mg g^{-1} for Zn^{2+}, Cu^{2+}, Pb^{2+}, Hg^{2+}, and Cd^{2+}, respectively. They reported that the synthesized chelating monolith can be easily regenerated by using 0.1 M HNO_3 with higher removal efficiency [46]. In another study, Wang and Zhang [47] synthesized a porous polymer-based monolith by *in-situ* polycondensation of epoxy monomer bisphenol A diglycidyl ether and ethylenediamine in the presence of pore-forming reagent (polyethylene glycol), and used it for the preconcentration and determination of Pb^{2+} ions using flame atomic absorption spectroscopy. The authors found that the maximum adsorption capacity of Pb^{2+} ions onto the formed monolith was 106.8 mg g^{-1}. They reported that the formed monolith exhibited superior reusability and stability. They concluded that the formed monolith is suitable for the preconcentration of Pb^{2+} ions as an ion-selective solid-phase extraction adsorbent [47].

The present work focuses on the preparation of a macroporous polyacrylamide-based monolith bearing negatively charged interaction sites (sulfonic acid groups) as a new adsorbent for the effective removal of Pb^{2+}, Cd^{2+}, and Cr^{3+} ions from aqueous solutions. Vinylsulfonic acid (VSA) was selected as an anionic monomer to introduce a negative charge on the surface of the resulting monolith that forms a complex with investigated metal ions. To the best of the author's knowledge, this is the first study of its kind to investigate the performance of anionic polyacrylamide-based monolith as an adsorbent for the removal of toxic heavy metals from aqueous solution. The monolith is prepared by copolymerization of the formed soluble inclusion complex (*N-tert*-butyl acrylamide/methylated β-cyclodextrin, 1:1 molar ratio) with VSA, piperazinediacrylamide (PDA), and methacrylamide in aqueous phosphate buffer (0.1 M, pH 7.0) inside a glass tube. The influences of pH, contact time, monolith dosage, initial concentration, and temperature for removal of Pb^{2+}, Cd^{2+}, and Cr^{3+} ions were determined using the batch equilibrium method. The experimental adsorption data were analyzed based on adsorption isotherm models such as Langmuir, Freundlich, and Dubinin–Radushkevich (D–R). The adsorption kinetic studies were explained by pseudo-first-order and pseudo-second-order kinetic models. The adsorption thermodynamic and adsorption kinetic constant values were also determined.

2. Experimental

2.1. Chemicals and instruments

All chemicals were analytical grade reagents and used without further purification. *N*,*N*,*N*′,*N*′-tetramethylethylendiamine (TEMED), di-sodium hydrogen phosphate dihydrate, ammonium sulfate (AS), hydrochloric acid (37%, v/v), and methanol were from Fluka (Buchs, Switzerland). VSA (25% w/v in aqueous solution), ammonium persulfate (APS) were from Sigma Aldrich (Steinheim, Germany). Methacrylamide (MA), sodium dihydrogen phosphate monohydrate were from Merck (Darmstadt, Germany). PDA was from Alfa-Aesar (Karlsruhe, Germany). Methylated β-CD (Me-β-CD) was from Sigma Aldrich (Louis, USA). Cadmium(II) nitrate tetrahydrate ($Cd(NO_3)_2{\cdot}4H_2O$), lead(II) chloride ($PbCl_2$), and chromium(III) nitrate ($Cr(NO_3)_3$) were from BDH Chemicals Ltd., Poole (England).

Filtration of solutions was done using nylon syringe filters 0.45 μm. The pH of metal ion solutions was measured using EUTECH pH-meter (Japan). Sample solutions were shaken using GFL-85 thermostatic mechanical shaker (250 rpm). The concentrations of the metal ions (Cd^{2+}, Cr^{3+}, and Pb^{2+}) in aqueous samples were determined using flame atomic absorption spectrophotometer (FAAS) (Anal Jena, AG, model: NOVAA300) with an auto sampler model (Type: AS 51S, U: 24V DC APP-Nr-:402071) equipped with a deuterium background correction. Analysis using FAAS was carried out at the most sensitive analytical spectral lines of the metals (Pb: 283.31 nm, Cr: 357.9 nm, and Cd: 228.8 nm).

2.2. Synthesis of the polyacrylamide-based monolith

The macroporous polyacrylamide-based monolith used in this work was synthesized as described in [45] with some minor modifications. The modified detailed synthesis procedures were described in our very recently published work [51]. Briefly, monolith synthesis was performed in a glass tube by copolymerization of the formed soluble inclusion complex (0.3 g *N-tert*-butylacrylamide/3.0 g methylated β-cyclodextrin) with 100 μL of 25% (w/v) VSA, 0.5 g PDA, 0.2 g MA, 0.2 g AS, 20 μL of 20% (w/v) APS, and 20 μL of 20% (v/v) TEMED in 0.1 M aqueous phosphate buffer (pH 7.0). The glass tube was then closed and the polymerization reaction was allowed to proceed overnight at room temperature (25°C).

2.3. Calibration curves

A 1,000 mg L^{-1} stock solution of each metal ion was prepared separately by dissolving the exact amounts of Pb^{2+}, Cd^{2+}, and Cr^{3+} in 1,000 mL of ultrapure deionized water. A series of freshly prepared working standard solutions with different concentrations for Pb^{2+}, Cd^{2+}, and Cr^{3+} were prepared by diluting an appropriate aliquot of the prepared stock solution for each metal ion using ultrapure deionized water for constructing the calibration curves. The pH of solutions was adjusted by using 0.2 mol L^{-1} NaOH or HCl for all batch experiments. The linear least-squares method was employed for the calculation of statistical parameters for each metal ion including the regression equation and correlation coefficient (R^2).

2.4. Determination of metal ions

An aliquot of filtrate solution containing Pb^{2+}, Cd^{2+}, or Cr^{3+} ions was quantitatively transferred into a volumetric flask and diluted (if necessary). Then, the concentration of unabsorbed metal ion left in the solution was determined by flame atomic absorption spectrometry (FAAS).

2.5. Batch adsorption experiments

Adsorption experiments for the investigated metal ions onto the monolith were investigated using the batch equilibrium technique. With the aim to optimize the experimental parameters for better Cd^{2+}, Pb^{2+}, and Cr^{3+} removal percentage, the adsorption process of each metal ion was studied as a function of pH, contact time, monolith dosage, initial concentration, and temperature.

2.5.1. Effect of pH

For each studied metal ion, a mass of 10 mg of the monolith was added to several 250 mL plastic bottles containing 25.0 mL of either 8 mg L^{-1} (Cd^{2+}), 15 mg L^{-1} (Cr^{3+}), or 30 mg L^{-1} (Pb^{2+}) solutions. The pH of each metal ion solution was adjusted over the pH range 3–6 using either 0.2 mol L^{-1} HCl or NaOH solutions (before the addition of the monolith). The bottles were then closed and placed in the shaker at 25°C for 24 h to reach equilibrium. The suspensions were then filtered, and the supernatants were analyzed for unabsorbed metal ions by FAAS.

2.5.2. Effect of monolith dosage

A mass of 5, 10, 15, 20, and 25 mg of the monolith were added to several 250 mL plastic bottles containing 25.0 mL of either 8 mg L^{-1} (Cd^{2+}), 15 mg L^{-1} (Cr^{3+}), or 30 mg L^{-1} (Pb^{2+}) solutions at pH 4. The bottles were then closed and placed in the shaker at 25°C for 24 h to reach equilibrium. The suspensions were then filtered, and the supernatants were analyzed for unabsorbed metal ions by FAAS.

2.5.3. Effect of contact time

A mass of 10 mg of the synthesized monolith was transferred to a number of 250 mL plastic bottles containing 25.0 mL of either 8 mg L^{-1} (Cd^{2+}), 15 mg L^{-1} (Cr^{3+}), or 30 mg L^{-1} (Pb^{2+}) solutions at pH 4 and 25°C. The bottles were then closed and placed in the shaker for different time intervals (1, 2, 4, 7, and 24 h). At the selected time for each bottle, the suspensions were filtered, and the supernatants were analyzed for unabsorbed metal ions by FAAS.

2.5.4. Effect of initial concentration

The effect of initial metal ion concentration on the removal percentage was studied by adding 25.0 mL of either (2–20 mg L^{-1}) for Cd^{2+}, (5–50 mg L^{-1}) for Cr^{3+}, or (5–60 mg L^{-1}) for Pb^{2+} solutions to several 250 mL plastic bottles containing 10 mg of the formed monolith at pH 4 and 25°C, 35°C, and 45°C. The bottles were then closed and placed in the shaker for 24 h to reach equilibrium. The suspensions were then filtered, and the supernatants were analyzed for unabsorbed metal ions by FAAS.

2.5.5. Effect of temperature

The effect of temperature on the removal percentage of Pb^{2+}, Cd^{2+}, and Cr^{3+} ions was studied by adding 25.0 mL of either 8.0 mg L^{-1} for Cd^{2+}, 15 mg L^{-1} for Cr^{3+}, or 30 mg L^{-1} for Pb^{2+} solutions to several 250 mL stopper plastic bottles containing 10 mg of the formed monolith at pH 4 with varying temperatures 25°C, 35°C, and 45°C. The bottles were then closed and placed in the shaker for 24 h to reach equilibrium. The suspensions were then filtered, and the supernatants were analyzed for unabsorbed metal ions by FAAS.

2.6. Adsorption experiments: kinetics and isotherms

The kinetics studies were carried out at 25°C, 35°C, and 45°C (pH 4). The pH values of metal ion solutions were adjusted at pH 4 by adding either 0.2 mol L^{-1} NaOH or HCl. Suspensions of 10 mg of the monolith in 25.0 mL of 8, 15, and 30 mg L^{-1} of Cd^{2+}, Cr^{3+}, and Pb^{2+} solutions, respectively, were shaken and then filtered at different times 1, 2, 4, 7, and 24 h.

Adsorption isotherm experiments were performed at pH 4 at constant temperatures 25°C, 35°C, and 45°C. A mass of 10 mg of the formed monolith was introduced in metal ions solution (25.0 mL) of varying initial concentrations

(2–20 mg L^{-1}) for Cd^{2+}, (5–50 mg L^{-1}) for Cr^{3+}, and (5–60 mg L^{-1}) for Pb^{2+}. The suspensions were then shaken for 24 h to reach equilibrium and then filtered. Finally, the supernatants were analyzed for unabsorbed metal ions by FAAS.

In order to explain the experimental adsorption results obtained in this study, different isotherm models like Langmuir, Freundlich, and D–R were suggested. Data obtained from the analysis of these isotherm models gives information about the effectiveness of the synthesized monolith toward the removal of the investigated metal ions. Generally, the efficiency of the adsorption process can be estimated from the calculation of the adsorption capacity at equilibrium q_e (amount of metal ion adsorbed per mass unit of the monolith at equilibrium (mg g^{-1})), adsorption capacity at a specific time q_t (mg g^{-1}), and removal percentage (%R) using the following equations [20]:

$$q_e = \frac{\left(C_0 - C_e\right)}{m} V \tag{1}$$

$$q_t = \frac{\left(C_0 - C_t\right)}{m} V \tag{2}$$

$$\%R = \frac{\left(C_0 - C_e\right)}{C_0} \tag{3}$$

where C_0 is the initial concentration of a metal ion in the aqueous solution (mg L^{-1}), C_e is the equilibrium concentration of a metal ion in the aqueous solution (mg L^{-1}), C_t is the concentration of a metal ion in the aqueous solution (mg L^{-1}) at time t, m is the adsorbent mass (mg), and V is the volume of the aqueous solution (L).

3. Results and discussion

3.1. Adsorption studies

3.1.1. Effect of solution pH

In the adsorption process, the solution pH has a significant impact on the adsorption efficiency by influencing the surface charge of the adsorbent (i.e., degree of ionization of groups present on the adsorbent surface) and precipitation of metal ion in an aqueous solution [29,39,52]. In this study, the impact of solution pH on the removal of Cd^{2+}, Pb^{2+}, and Cr^{3+} ions was investigated over the range from 3.0 to 6.0. The adsorption of metal ions at pH higher than 6 was not considered because the precipitation of metal ions as insoluble metal hydroxide becomes significant at approximately pH 7.0 [46,53]. As can be seen from Fig. 1a, the removal percentage of the studied metal ions increases with increasing the pH of the solution from 3 to 6. This observation can be explained by the increase in the number of the negatively charged sulfonic acid groups per surface unit monolith that form a complex with metal ions. It can be seen that the maximum removal percentage was observed at pH 6 for all metal ions. At low pH values (pH < 3), adsorption occurred with low removal percentage for the investigated metal ions. This is because, at low pH, the surface of the monolith was covered by H^+ ions, which restricted metal cations approach to the negatively charged sulfonic acid groups present on the monolith surface through electrostatic repulsion, and thereby results in the decrease of the removal percentage of the investigated metal ions [39]. As the solution pH is increased (pH > 4), the concentration of H^+ ions decreases in the aqueous solution and the monolith surface becomes negatively charged. Consequently, the electrostatic repulsion that exists between metal cations in the bulk solution and H^+ ions on the monolith surface decreases and thereby results in the increase of the removal percentage of the investigated metal ions. In addition, Fig. 1a shows that the removal percentage of metal ions at the optimum pH increases in the order of $Cd^{2+} > Cr^{3+} > Pb^{2+}$.

3.1.2. Effect of monolith dosage

As the second step, we have investigated the influence of the mass of the monolith on the removal percentage of Cd^{2+}, Cr^{3+}, and Pb^{2+} ions. In general, the mass of adsorbent plays an important role in the adsorption process, since it determines the number of available active sites present in the adsorbent. As can be seen from Fig. 1b, there is an increase in the removal percentage of Cd^{2+}, Cr^{3+}, and Pb^{2+} ions with increasing the mass of the monolith from 5 to 25 mg. For example, the removal percentage of Cr^{3+} increases from about 53% to 83% with increasing the mass of the monolith from 5 to 25 mg (Fig. 1b). The increase in the removal percentage of the studied metal ions with an increase in the monolith dosage can be attributed to the increase in the number of the available active sites (sulfonic acid groups) on the monolith surface and to the presence of a large surface area available for adsorption.

3.1.3. Effect of contact time

Contact time is an important and crucial experimental factor required for studying the adsorption kinetics of metal ions on the surface of the monolith. In this study, the effect of contact time was studied between 1 and 24 h for the adsorption of Cd^{2+}, Cr^{3+}, and Pb^{2+} ions onto the monolith. Results given in Fig. 1c demonstrate that the removal percentage of the investigated metal ions increased rapidly within the first 1–7 h and then reached the plateau value (i.e., equilibrium). For example, there is an increase in the removal percentage of more than 63%, 59%, and 58% for Cd^{2+}, Cr^{3+}, and Pb^{2+}, respectively, reached during the time interval 1–7 h. These results can be attributed to the availability of the free active sites (sulfonic acid groups) on the monolith surface. In addition, results show that increasing contact time above 7 h does not affect significantly the removal of the investigated metal ions, which might be attributed to the fewer sulfonic acid groups available on the monolith surface to interact with the metal ions. These findings indicate that equilibrium was established between the aqueous solution and the monolith. The obtained results reveal that the adsorption rate of Cd^{2+}, Cr^{3+}, and Pb^{2+} ions onto the monolith is moderately slow (i.e., needs 7 h to reach a saturation level), which implies that the adsorption of metal ions occurs on the surface of the monolith and in the internal mesopores and flow-through pores present

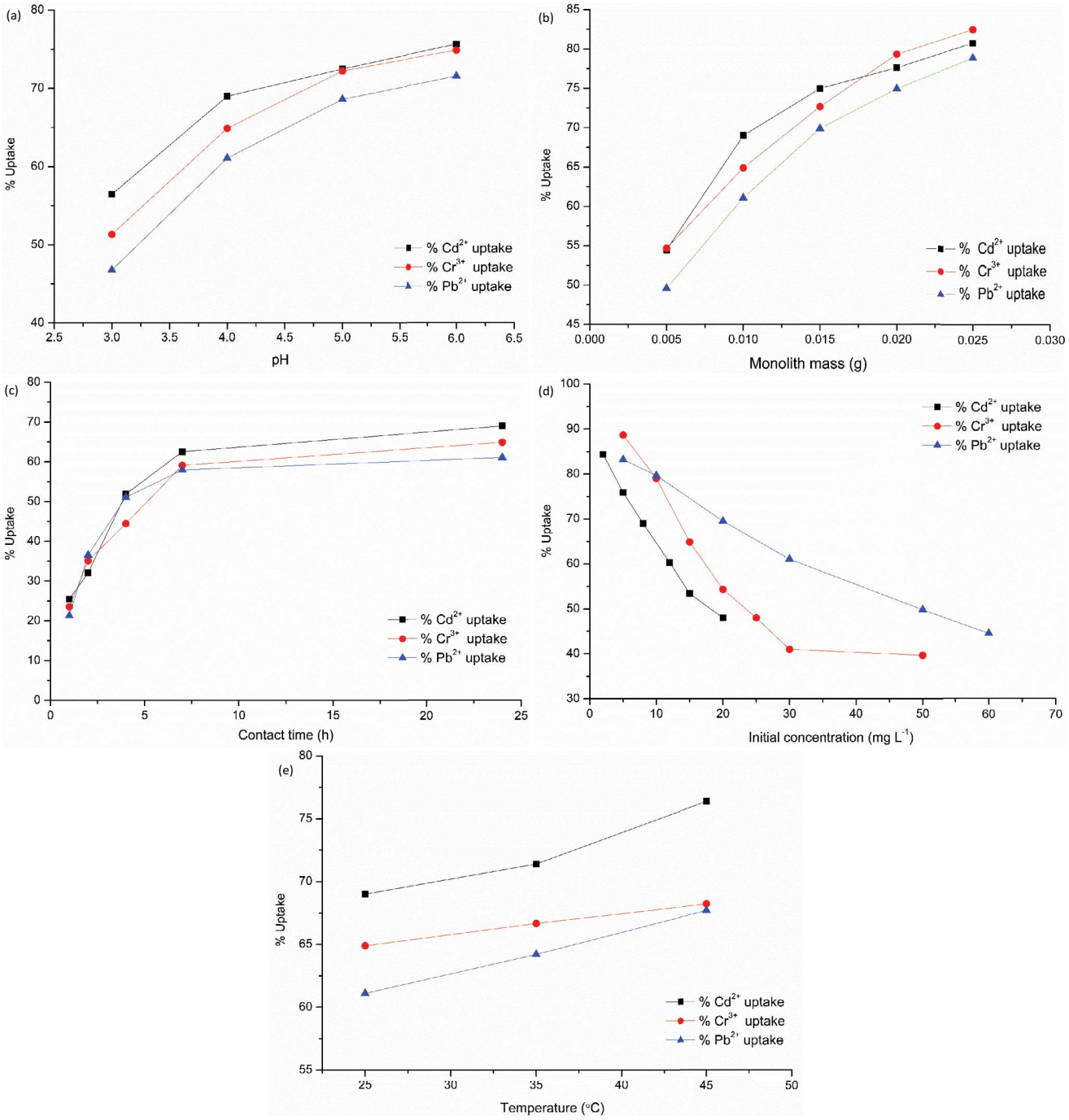

Fig. 1. Effect of various experimental conditions on the removal percentage of Cd^{2+}, Pb^{2+}, and Cr^{3+} ions including: effect of (a) pH, (b) monolith dosage, (c) contact time, (d) initial concentration, and (e) adsorption temperature.

within the monolithic scaffold. The maximum removal percentage obtained for Cd^{2+}, Cr^{3+}, and Pb^{2+} were 55%, 52%, and 50%, respectively.

3.1.4. Effect of initial concentration

The influence of initial concentration on the removal of the investigated metal ions was studied in the range of (2–20 mg L^{-1}) for Cd^{2+}, (5–50 mg L^{-1}) for Cr^{3+}, and (5–60 mg L^{-1}) for Pb^{2+} at pH 4 and 25°C, 35°C, 45°C. As can be seen from Fig. 1d, there is an increase in the removal percentage of Cd^{2+}, Cr^{3+}, and Pb^{2+} ions with decreasing their initial concentrations. For example, it is observed that an increase in the initial Cr^{3+} concentration from 5 to 50 mg L^{-1} leads to a decrease in the removal percentage from 89% to 40% for Cr^{3+} adsorbed on the monolith. These results can

be attributed to the saturation of the monolith surface at higher initial metal ion concentrations, which results in a clear decrease in the removal percentage of metal ions [32,54]. Furthermore, at high initial metal ion concentrations, the ratio of metal ions to the monolith mass is high, and hence more ions are bonded to the same number of active sites present on the monolith surface, which results in saturation of the monolith surface, and consequently, decreasing in the removal percentage of metal ions [32,54]. Whereas, at low initial metal ion concentrations, the ratio of metal ions to the monolith mass is low and more ions are adsorbed on the monolith surface causing an increase in the removal percentage of metal ions. In this context, several authors have reported an increase in removal percentage with decreasing initial concentration of adsorbate [32,54,55].

3.1.5. Effect of temperature

In this study, the effect of temperature on the removal of Cd^{2+}, Cr^{3+}, and Pb^{2+} ions was investigated at the temperature range of 25°C–45°C. As can be seen from Fig. 1e, there is an increase in the removal percentage of metal ions with increasing adsorption temperature from 25°C to 45°C. The increase in adsorption temperature enhances the electrostatic interaction between the negatively charged sulfonic acid groups and positively charged metal ions on the monolith surface and thereby results in the increase of the removal percentage of metal ions [54]. The increase in the removal percentage with an increase in the adsorption temperature indicates that the adsorption of Cd^{2+}, Cr^{3+}, and Pb^{2+} ions onto the monolith is an endothermic process.

3.2. Adsorption kinetics

Adsorption kinetics of metal ions are characterized by two steps: the initial step in which adsorption of metal ions onto the adsorbent surface is fast and mostly referred to as equilibrium uptake, and a second step in which adsorption of metal ions is being slower and referred to the adsorption of metal ions onto the adsorbent surface [20]. With the aim to study the kinetics of adsorption of Cd^{2+}, Cr^{3+}, and Pb^{2+} ions onto the formed monolith, the relationship between the adsorption capacity and equilibrium time was investigated at 25°C, 35°C, and 45°C. The experimental kinetic data obtained for Cd^{2+}, Cr^{3+}, and Pb^{2+} ions were analyzed using Lagergren pseudo-first-order and pseudo-second-order kinetic models [33,56,57]. The pseudo-first-order kinetic model is given by the following equation:

$$\ln\left(q_e - q_t\right) = \ln\left(q_e\right) - k_1 t \tag{4}$$

The pseudo-second-order kinetic model is given by the following equation:

$$\frac{t}{q_t} = \frac{1}{k_2 q_e^2} + \frac{1}{q_e} t \tag{5}$$

where q_e and q_t are the amounts of the adsorbed metal ion at equilibrium and at time t, respectively, t is the contact time (min), k_1 is the rate constant for pseudo-first-order reaction (min^{-1}) and k_2 is the rate constant for pseudo-second-order reaction (g mg^{-1} min^{-1}). The experimental kinetic data obtained for Cd^{2+}, Cr^{3+}, and Pb^{2+} ions were analyzed using the pseudo-first-order and pseudo-second-order kinetics models. Linear fit plots for these kinetic models are shown in Fig. 2. These fittings will allow estimating for Cd^{2+}, Cr^{3+}, and Pb^{2+} ions the calculated equilibrium adsorption capacity q_e^{cal}, the pseudo-first-order rate constant k_1, the pseudo-second-order rate constant k_2, the correlation coefficient R^2, and the reduced chi-square χ^2. All these calculated parameters for the studied kinetic models along with the values of the experimental equilibrium adsorption capacity q_e^{exp} for Cd^{2+}, Cr^{3+}, and Pb^{2+} ions are listed in Table 1. In this study, the values of correlation coefficient R^2 and reduced chi-square χ^2 were calculated and applied to evaluate the degree of goodness of fit between the proposed kinetics models and experimental kinetic data, and consequently, find out the suitable kinetic model that can be used for describing the experimental kinetic data. In general, the suitable kinetic model used for describing the experimental kinetic data is characterized by high R^2 and

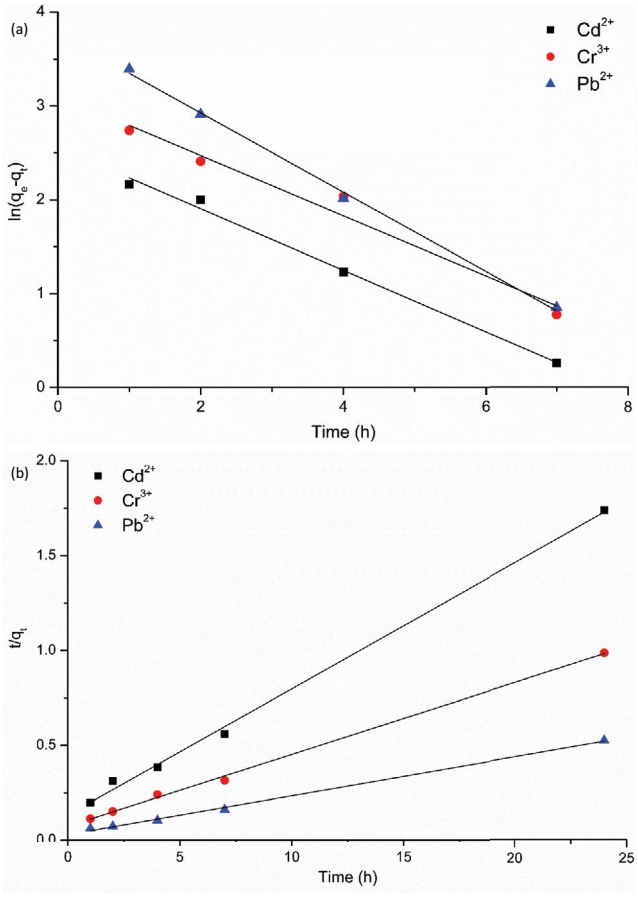

Fig. 2. (a) Pseudo-first-order and (b) pseudo-second-order kinetic models for the adsorption of Cd^{2+}, Pb^{2+}, and Cr^{3+} ions onto the polyacrylamide-based monolith at pH = 4.0, temperature = 25°C, contact time = 1–24 h, monolith dosage = 10 mg/25 mL, initial metal concentration = Cd^{2+} (8 mg L^{-1}), Cr^{3+} (15 mg L^{-1}), and Pb^{2+} (30 mg L^{-1}).

Table 1
Calculated parameters of pseudo-first-order and second-order kinetic models for the adsorption of Cd^{2+}, Cr^{3+}, and Pb^{2+} ions onto the polyacrylamide-based monolith at pH = 4.0, temperature = 25°C, 35°C, and 45°C, contact time = 1–24 h, monolith dosage = 10 mg/25 mL, initial concentration = Cd^{2+} (8 mg L^{-1}), Cr^{3+} (15 mg L^{-1}), and Pb^{2+} (30 mg L^{-1})

			Pseudo-first-order				Pseudo-second-order			
Metal ion	Temperature (°C)	q_e^{exp} (mg g^{-1})	q_e^{cal} (mg g^{-1})	k_1 (h^{-1})	R^2	χ^2	q_e^{cal} (mg g^{-1})	k_2 (g mg^{-1} h^{-1})	R^2	χ^2
Cd^{2+}	25	13.80	12.97	0.33	0.991	0.05	15.04	0.03	0.997	0.10
	35	14.28	12.74	0.34	0.991	0.19	15.38	0.04	0.998	0.08
	45	15.28	12.24	0.29	0.974	0.75	16.43	0.04	0.998	0.08
Cr^{3+}	25	24.33	22.54	0.32	0.961	0.14	26.41	0.02	0.998	0.16
	35	25.0	21.34	0.34	0.950	0.63	26.72	0.02	0.998	0.11
	45	22.58	19.38	0.32	0.960	1.99	27.08	0.03	0.999	0.08
Pb^{2+}	25	45.81	43.48	0.42	0.997	0.13	49.01	0.01	0.997	0.21
	35	48.15	37.79	0.36	0.985	2.84	51.02	0.02	0.999	0.16
	45	50.81	34.76	0.30	0.981	7.41	53.51	0.02	0.999	0.14

low χ^2 values. The reduced chi-square χ^2 is expressed by the following equation:

$$\chi^2 = \frac{\left(q_e^{exp} - q_e^{cal}\right)^2}{q_e^{cal}} \quad (6)$$

where q_e^{cal} is the calculated equilibrium adsorption capacity (mg g^{-1}) estimated from pseudo-first-order or pseudo-second-order kinetic rate equation and q_e^{exp} is the experimental equilibrium adsorption capacity (mg g^{-1}) calculated by using Eq. (1).

According to the results depicted in Table 1 and Fig. 2, the high R^2 (>0.997) and low χ^2 values obtained for the pseudo-second-order kinetic model compared to the pseudo-first-order model makes it the suitable kinetic model for describing the kinetic data for the metal ions adsorption onto the monolith. In addition, results in Table 1 demonstrate that the q_e^{cal} values estimated from the pseudo-second-order equation were in good agreement with the q_e^{exp} values for Cd^{2+}, Cr^{3+}, and Pb^{2+} ions compared to the pseudo-first-order kinetic model. These findings confirm that the pseudo-second-order is the suitable kinetic model used to describe the kinetic of adsorption of the metal ions onto the synthesized monolith. These results suggest that the adsorption process for Cd^{2+}, Cr^{3+}, and Pb^{2+} ions onto the monolith is controlled by chemisorption. Similar results have been reported by authors working on the adsorption of metal ions onto ion-imprinted polymer-based monoliths [48], porous carbon monolith [29], and silica-based monoliths [39].

3.3. Adsorption isotherms

3.3.1. Adsorption isotherm curves

Adsorption isotherm results obtained for Cd^{2+}, Cr^{3+}, and Pb^{2+} ions are shown in Fig. 3. As a general trend, the adsorption capacity (q_e) increased with increasing equilibrium concentration (C_e), which might be explained by the increase in the initial metal ion concentration. In general, the increase in initial metal ion concentration results in an increase in the electrostatic interaction between the negatively charged sulfonic acid groups and metal ion on the monolith surface and thereby results in the increase of the adsorption capacity of the metal ion. We also observed that the isotherm curves obtained for Cd^{2+}, Cr^{3+}, and Pb^{2+} do not reach a plateau value as equilibrium concentration increases, which implies that the monolayer for each studied metal ion was not completely formed on the monolith surface (Fig. 3). According to Giles and Smith's [58] isotherms classification, the shape of the isotherm curves obtained for the studied metal ions indicates L1-type adsorption isotherm (i.e., normal Langmuir isotherms). L1-type isotherms are usually used to describe the adsorption behavior of charged solutes (e.g., metal ions and ionic organic molecules) with no strong competition with solvent molecules to occupy the available active sites on the adsorbent surface. According to L1-type, the adsorption of metal ions on the adsorbent surface involves a monolayer coverage [58]. In addition, the formation of multi-layers of the metal ions on the monolith surface was not possible due to the significant electrostatic repulsion forces between adsorbed metal ions and those present in the bulk solution [58]. The results depicted in Fig. 3 show that the adsorption capacity of Cd^{2+}, Cr^{3+}, and Pb^{2+} ions increases with increasing temperature, indicating that the adsorption of metal ions onto the monolith was an endothermic process. The increase in the adsorption capacity of metal ions with increasing temperature might be explained by the increase in the diffusion of metal ions from the bulk solution to the monolith surface and to the internal mesopores and flow-through pores present within the monolithic scaffold. In addition, results in Fig. 3 demonstrate that the adsorption temperature has no significant influence on the shape of the adsorption isotherm curves obtained for Cd^{2+} and Pb^{2+} ions (Figs. 3a and b). Whereas, for Cr^{3+} ions, there is a slight change in the upper part of the isotherm curve observed at higher metal equilibrium concentration, so that it changes from L1 to L3-type [58] (Fig. 3c). This behavior might be attributed to the change

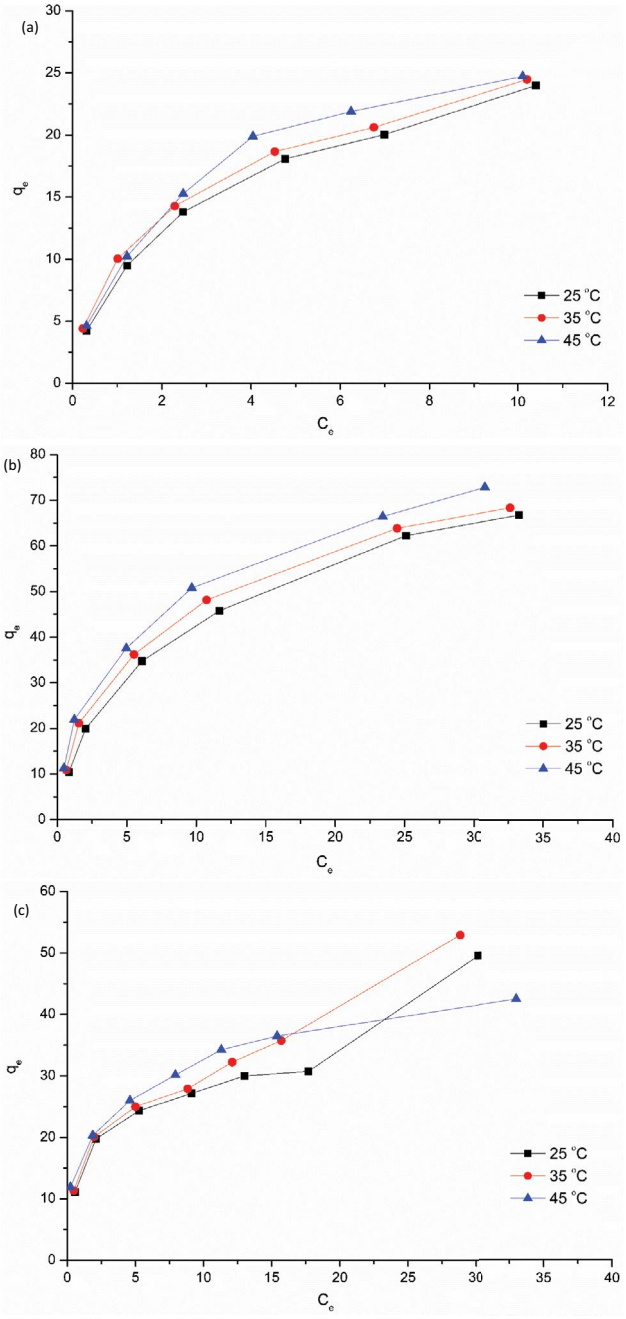

Fig. 3. Adsorption isotherms of (a) Cd^{2+}, (b) Pb^{2+}, and (c) Cr^{3+} ions onto the polyacrylamide-based monolith at pH = 4.0, temperature = 25°C, 35°C, and 45°C, contact time = 24 h, monolith dosage = 10 mg/25 mL, initial concentration range = Cd^{2+} (2–20 mg L^{-1}), Cr^{3+} (5–50 mg L^{-1}), and Pb^{2+} (5–60 mg L^{-1}).

in the adsorption behavior exhibited by Cr^{3+} ions due to its relatively large charge compared to Cd^{2+} and Pb^{2+} ions.

3.3.2. Langmuir, Freundlich, and D–R isotherms

It is well-known that adsorption isotherms play important role in understanding the adsorption mechanism of the adsorbate and also to quantify the experimental adsorption capacity (q_e^{exp}) of the adsorbent [20,21,25]. For this purpose, the equilibrium experimental data (q_e and C_e) obtained for Cd^{2+}, Pb^{2+}, and Cr^{3+} ions were modeled with the linearized equations of the Langmuir, Freundlich, and D–R isotherm models [21,25,28]. This modeling will allow estimating for each isotherm model the fitting parameters, and consequently, find out the most suitable isotherm model that can be used for describing the experimental equilibrium data. The Langmuir adsorption isotherm is usually used for monolayer adsorption [28]. This model assumes that all the adsorption sites are identical and that the binding energy of these adsorption sites is equal (i.e., homogenous adsorption) [28]. The linearized equation of the Langmuir isotherm model is expressed as [20,21,28]:

$$\frac{1}{q_e}=\left(\frac{1}{q_{\max}K_L}\right)\frac{1}{C_e}+\frac{1}{q_{\max}} \tag{7}$$

where $q_{\max}$ is the maximum amount of metal ion adsorbed per mass unit of the monolith at monolayer coverage (mg g^{-1}), K_L is the Langmuir constant that relates to the energy of the adsorption process (L mg^{-1}) [21]. The values of K_L and $q_{\max}$ are calculated using the values of the slope and intercept of the linear plot of $1/q_e$ vs. $1/C_e$ as shown in Figs. 4–6. The separation factor or called equilibrium parameter R_L is then calculated according to the following equation:

$$R_L=\frac{1}{1+K_LC_0} \tag{8}$$

The separation factor R_L was the essential characteristic of the Langmuir isotherm model that was used to predict the favorability of the adsorption process. The value of R_L indicates the adsorption process to be favorable when $0 < R_L < 1$, unfavorable when $R_L > 1$, linear when $R_L = 1$, and irreversible when $R_L = 0$ [20,52,59].

Freundlich isotherm is an empirical model used to describe the surface heterogeneity and the non-uniform distribution of active sites and their energies on the adsorbent surface. This model can be applied to multilayer adsorption. The linearized equation of the Freundlich isotherm model can be expressed as [21,28]:

$$\log q_e=\log K_F+\frac{1}{n}\log C_e \tag{9}$$

where K_F (L mg^{-1}) is the Freundlich constant represents the adsorption capacity and n (heterogeneity factor) is the empirical constant represents the intensity of the adsorption process. The values of n indicate the adsorption process is normal when $n > 1$ and cooperative adsorption when $n < 1$ [20]. The values of K_F and n can be easily calculated using the values of the slope and intercept of the linear plot of $\log q_e$ vs. $\log C_e$ as shown in Figs. 4–6.

D–R isotherm model was used to find the potential binding energy E (kJ mol^{-1}) that describes the movement

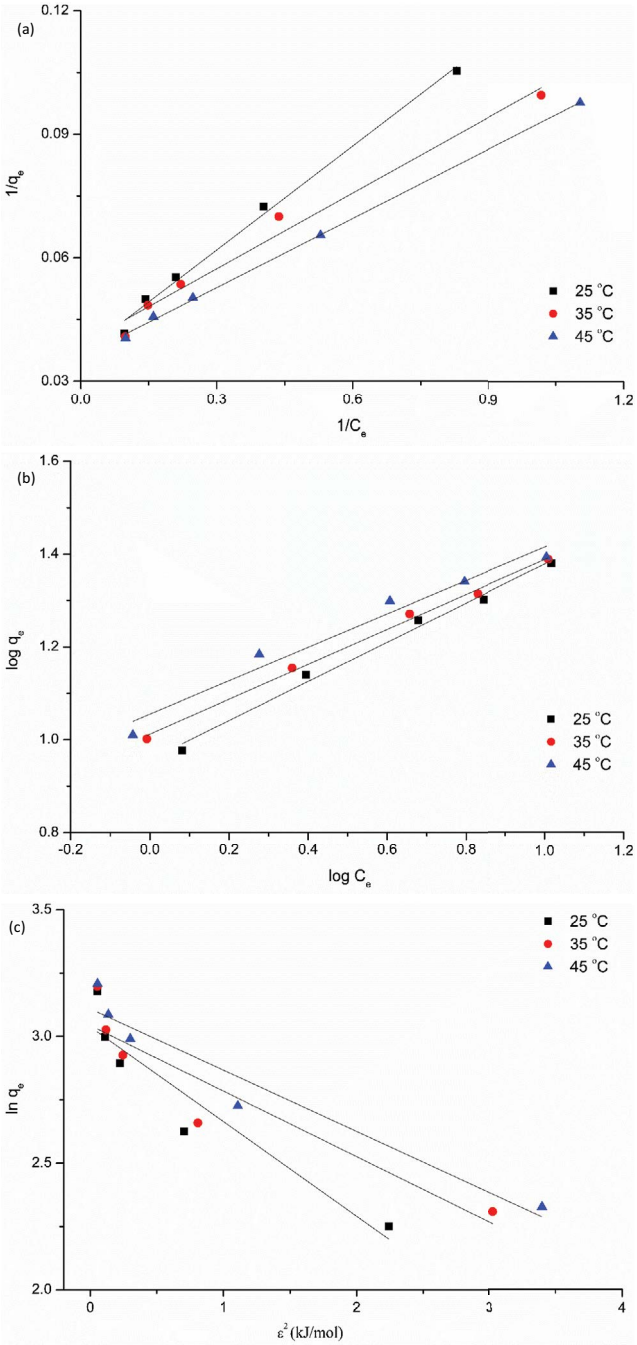

Fig. 4. Plots of linearized adsorption isotherm of Cd^{2+} ions onto the polyacrylamide-based monolith: (a) Langmuir model, (b) Freundlich model, and (c) D–R model at pH = 4.0, temperature = 25°C, 35°C, and 45°C, contact time = 24 h, monolith dosage = 10 mg/25 mL, and metal concentration range = Cd^{2+} (2–20 mg L^{-1}).

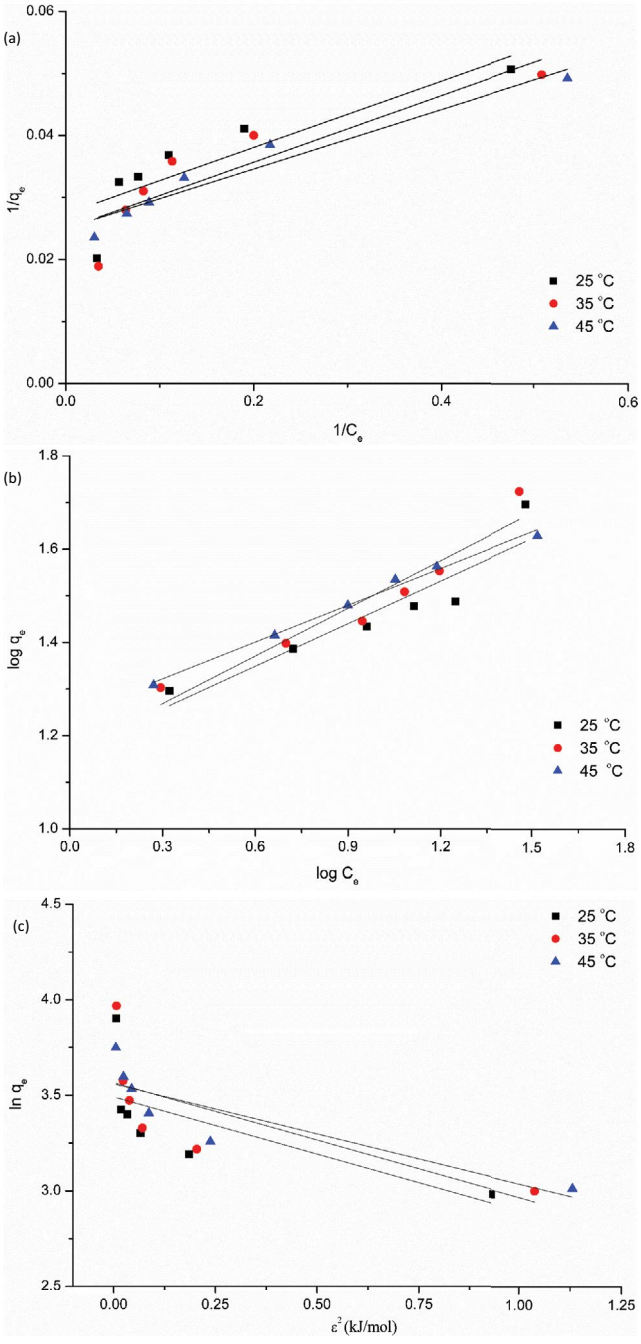

Fig. 5. Plots of linearized adsorption isotherm of Cr^{3+} ions onto the polyacrylamide-based monolith: (a) Langmuir model, (b) Freundlich model, and (c) D–R model at pH = 4.0, temperature = 25°C, 35°C, and 45°C, contact time = 24 h, monolith dosage = 10 mg/25 mL, and metal concentration range = Cr^{3+} (5–50 mg L^{-1}).

of one mole of adsorbate from an aqueous solution to an adsorbent surface. The liner form of the D–R model is given by the following equation [28]:

$$\ln\left(q_e\right) = \ln\left(q_{\max}\right) - \beta\varepsilon^2 \tag{10}$$

$$\varepsilon = RT\ln\left(1+\frac{1}{C_e}\right) \tag{11}$$

where R is the gas constant (J K^{-1} mol^{-1}), T is the temperature (K), ε is the Polanyi potential, β (mol^2 kJ^{-2}) is the

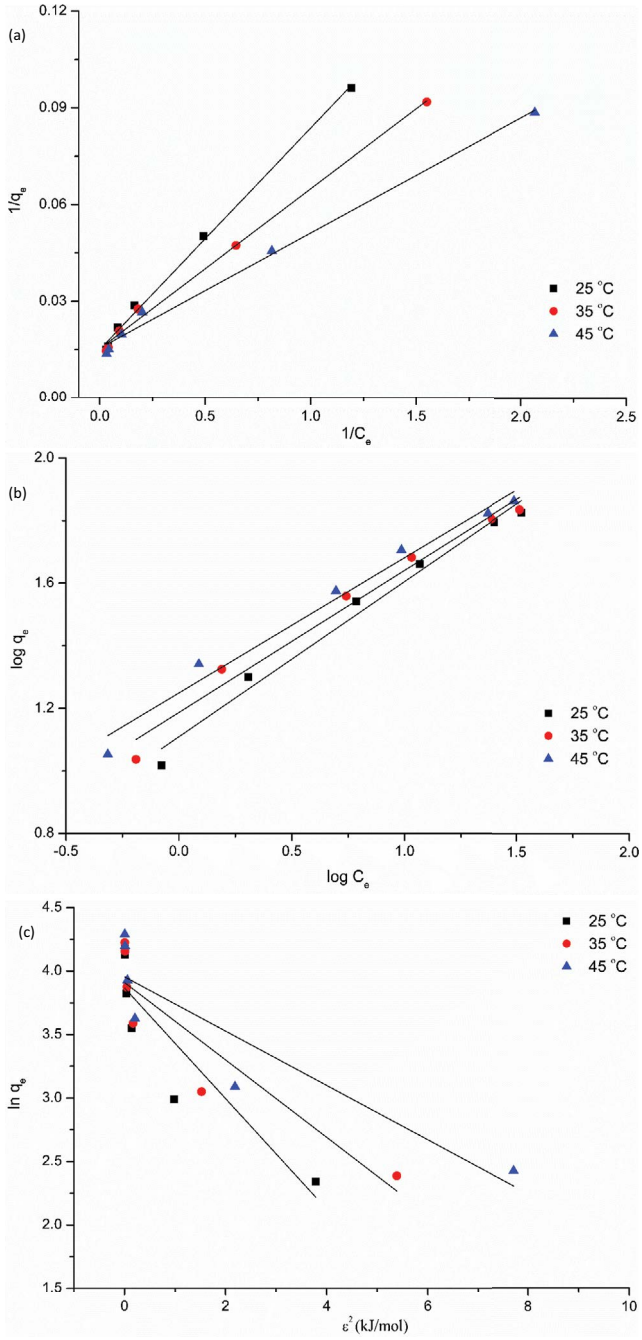

Fig. 6. Plots of linearized adsorption isotherm of Pb^{2+} ions onto the polyacrylamide-based monolith: (a) Langmuir model, (b) Freundlich model, and (c) D–R model at pH = 4.0, temperature = 25°C, 35°C, and 45°C, contact time = 24 h, monolith dosage = 10 mg/25 mL, and metal concentration range = Pb^{2+} (5–60 mg L^{-1}).

activity coefficient that relates to mean adsorption energy, E (kJ mol^{-1}) represents the potential binding energy that describes the movement of one mole of adsorbate from the bulk solution to the adsorbent surface. E can be calculated using the following equation:

$$E = \frac{1}{\sqrt{2\beta}} \tag{12}$$

Plots for the Langmuir, Freundlich, and D–R isotherm models for the adsorption of Cd^{2+}, Cr^{3+}, and Pb^{2+} ions onto the monolith at studied temperatures are shown in Figs. 4–6. In addition, Table 2 illustrates the Langmuir, Freundlich, and D–R fitting parameters together with R^2 and χ^2 values.

Linearized plots for the Langmuir and Freundlich models for the adsorption of Cd^{2+}, Pb^{2+}, and Cr^{3+} ions onto the monolith are shown to be linear with high R^2 values (Figs. 4–6). In the literature, it is accepted that the adsorption process fits the Langmuir and Freundlich isotherm models when the R^2 values are greater than 0.89 [60,61]. The results given in Table 2 show that the R^2 values are found to be greater than 0.91 for the Langmuir and Freundlich models, which confirms that these models can adequately describe the adsorption process of the studied metal ions onto the synthesized monolith due to the presence of homogeneous and heterogeneous sites. Furthermore, the results indicated that the Langmuir model was well-fitted to explain the metal ions adsorption onto the monolith surface due to the better R^2 for this adsorption model. Compared with the Langmuir and Freundlich isotherm models, the D–R adsorption isotherm is a less suitable model for describing the adsorption process of the investigated metal ions onto the monolith. It was found that the R^2 values obtained for the D–R model are less than 0.86 (Table 2).

The results given in Table 2 show that the R_L values estimated from the Langmuir isotherm model were ranged between 0 and 1, indicating the favorable adsorption of Cd^{2+}, Pb^{2+}, and Cr^{3+} ions by the formation of the monolayer at the monolith surface (Table 2). The maximum monolayer adsorption capacities for Cd^{2+}, Pb^{2+}, and Cr^{3+} ions onto the monolith were found to be 22.8, 33.3, and 66.7 mg g^{-1}, respectively (Table 2). In this context, the maximum adsorption capacity values of Cd^{2+}, Pb^{2+}, and Cr^{3+} on the synthesized monolith have been compared with those of other adsorbents reported in the literature (Table 3). It can be seen that the synthesized monolith had a slightly lower adsorption capacity in comparison to these adsorbents, which might be attributed to different experimental conditions.

According to the results depicted in Table 2, the K_L values obtained for the investigated metal ions show that Cr^{3+} ions exhibited higher values than that of Cd^{2+} and Pb^{2+} ions. For example, the values of K_L were found to be 0.43, 1.90, 2.44 L mg^{-1} for Pb^{2+}, Cd^{2+}, and Cr^{3+} at 45°C, respectively. This implies that the adsorption of Cr^{3+} ions onto the monolith surface was more favorable compared to Cd^{2+} and Pb^{2+} ions. These results can be explained based on the charge of metal ion so that metal ion with a higher charge forms a strong electrostatic interaction with the negatively charged sulfonic acid groups present on the monolith surface.

According to the Freundlich isotherm model, the value of the heterogeneity factor (n) measures the deviation from the linearity of the adsorption process. Adsorption is described as a chemical process if n = 1.0, and as a physical

Table 2
Isotherm parameters obtained for Langmuir, Freundlich, and D–R isotherm models calculated at different temperatures for Cd^{2+}, Cr^{3+}, and Pb^{2+} ions at pH = 4.0, temperature = 25°C, 35°C, and 45°C, contact time = 24 h, monolith dosage = 10 mg/25 mL, metal concentration range = Cd^{2+} (2–20 mg L^{-1}), Cr^{3+} (5–50 mg L^{-1}), and Pb^{2+} (5–60 mg L^{-1})

Metal	Cd^{2+}			Cr^{3+}			Pb^{2+}		
T (°C)	25	35	45	25	35	45	25	35	45
q_e^{exp} (mg g^{-1})	24.0	24.49	24.73	49.58	52.92	42.50	66.77	68.40	72.90
Langmuir isotherm									
q_{max} (mg g^{-1})	22.83	21.98	20.70	33.33	34.72	32.26	66.67	65.36	64.94
K_L (L mg^{-1})	0.72	1.06	1.90	0.86	1.00	2.44	0.22	0.31	0.43
R_L	0.07	0.05	0.03	0.02	0.02	0.01	0.07	0.05	0.04
R^2	0.99	0.99	0.97	0.95	0.93	0.91	0.99	0.99	0.99
χ^2	0.06	0.29	0.78	7.92	9.54	3.25	0.00	0.14	0.98
Freundlich isotherm									
K_F (L mg^{-1})	8.10	9.22	10.61	13.84	14.68	17.50	12.85	15.37	17.74
n	2.04	2.24	2.46	3.06	2.94	3.80	2.02	2.20	2.31
R^2	0.99	0.98	0.98	0.95	0.97	0.99	0.98	0.98	0.98
Dubinin–Radushkevich (D–R) isotherm									
q_{max} (mg g^{-1})	17.86	18.38	18.84	30.26	32.04	31.36	47.82	49.93	52.22
β (mol^2 kJ^{-2})	0.12	0.09	0.06	0.17	0.13	0.06	0.44	0.31	0.21
E (kJ mol^{-1})	2.05	2.40	2.90	1.74	1.96	2.90	1.07	1.27	1.53
R^2	0.86	0.87	0.85	0.71	0.69	0.74	0.82	0.84	0.84
χ^2	2.12	2.03	1.90	12.33	13.61	3.96	7.51	6.82	8.19

Table 3
Comparative account of the adsorption capacity of heavy metals (Cd^{2+}, Pb^{2+}, and Cr^{3+}) by different adsorbents

Adsorbent	Metal ion	q_e (mg g^{-1})	Conditions	References
SiO_2 monolith	Pb^{2+}	125	pH = 6.0	[39]
	Cd^{2+}	91	Temperature = 30°C	
MnO_2 monolith	Pb^{2+}	200	Time = 80 min	
	Cd^{2+}	125		
TiO_2 monolith	Pb^{2+}	857		
	Cd^{2+}	770		
Carbon monolith	Pb^{2+}	1,128	pH = 6.0	[29]
	Cd^{2+}	989	Temperature = 30°C	
			Time = 150 min	
Poly(hydroxyethyl methacrylate) monolith	Pb^{2+}	246	pH = 6.0	[46]
	Cd^{2+}	284	Temperature = 20°C	
Zinc NPs impregnated cellulose	Cr^{3+}	83	pH = 5.5	[31]
	Pb^{2+}	44	Temperature = 25°C	
Sliver NPs impregnated cellulose	Cr^{3+}	158	Time = 400 min	
	Pb^{2+}	85		
Activated carbon/zirconium oxide composite	Cd^{2+}	167	pH = 6.0	[25]
			Temperature = 25°C	
			Time = 120 min	
Polyacrylamide-based monolith	Cd^{2+}	23	pH = 4.0	Present study
	Pb^{2+}	33	Temperature = 25°C	
	Cr^{3+}	67	Time = 24 h	

process if $n > 1.0$ [61]. Results given in Table 2 show that the n values obtained for Pb^{2+}, Cd^{2+}, and Cr^{3+} ions were greater than 1.0, which reflects the favorable physical adsorption of the investigated metal ions onto the monolith [52]. In addition, the results presented in Table 2 showed that the values of Freundlich constant (K_F) for Pb^{2+}, Cd^{2+}, and Cr^{3+} ions increased with increasing the temperature, which confirmed the endothermic nature of metal ions adsorption onto the monolith surface [25]. For example, K_F for Pb^{2+} increases from about 12.85 L mg^{-1} at 25°C to about 15.37 L mg^{-1} at 35°C and increases further to about 17.74 L mg^{-1} at 45°C (Table 2). The same trend was observed for Cd^{2+} and Cr^{3+} ions (Table 2).

The results obtained from the Langmuir and Freundlich isotherm models suggest the formation of a monolayer of Pb^{2+}, Cd^{2+}, and Cr^{3+} ions onto the monolith surface by a physical electrostatic interaction between these metal ions and the negatively charged sulfonic acid groups present on the monolith surface (i.e., ion-exchange mechanism). Then, the formed monolayer forms multi-layers by chemical bonding with metal ions present in the bulk solution [20,51]. The results summarized in Table 2 show that the values of binding energy (E) obtained from the D–R model were less than 8 kJ mol^{-1} at the studied temperatures, which confirms the physical adsorption of the metal ions onto the monolith surface [52]. In the literature, it is reported that physical adsorption occurs with bond strengths less than 84 kJ mol^{-1}, while chemical adsorption bond strengths can range from 84 to 420 kJ mol^{-1} [30]. These findings also confirm the physical adsorption of the investigated metal ions on the monolith surface.

Another characteristic observation shown in Table 2 is that values of q_{max} evaluated using the Langmuir model are larger than those evaluated using the D–R model [52,62]. This difference might be stemmed from the definition of q_{max} in the two isotherm models. According to the Langmuir isotherm model, q_{max} represents the maximum adsorption capacity of adsorbate at monolayer coverage, whereas, in the D–R model, q_{max} represents the maximum adsorption capacity of adsorbate at the total accessible pores volume of the adsorbent. In this study, the values of q_{max} evaluated using the Langmuir isotherm model were adopted to describe the adsorption process of Pb^{2+}, Cd^{2+}, and Cr^{3+} ions onto the monolith due to the high R^2 and low χ^2 values (Table 2).

Results in Table 2 demonstrate that there is a slight decrease in the values of q_{max} (evaluated using the Langmuir isotherm model) for Pb^{2+}, Cd^{2+}, and Cr^{3+} ions with increasing temperature. For example, q_{max} for Cd^{2+} decreases from about 22.83 mg g^{-1} at 25°C to about 21.98 mg g^{-1} at 35°C and decreases further to about 20.70 mg g^{-1} at 45°C (Table 2). The same trend was observed for Cr^{3+} and Pb^{2+} ions. These findings indicate that the adsorption of the investigated metal ions onto the monolith is an exothermic process and becomes unfavorable as the adsorption temperature increases. On the other side, results in Table 2 show that there is an increase in the values of q_{max} evaluated using the D–R model with increasing temperature. For example, q_{max} for Pb^{2+} increases from about 47.82 mg g^{-1} at 25°C to about 49.93 mg g^{-1} at 35°C and increases further to about 52.22 mg g^{-1} at 45°C (Table 2). The same trend was observed for Cr^{3+} and Cd^{2+} ions. These results indicate that the adsorption of the studied metal ions onto the synthesized monolith is an endothermic process.

3.4. Thermodynamic studies

It is known that spontaneity of the adsorption process can be determined by evaluation of several thermodynamic parameters including standard Gibbs free energy change $\Delta G°$ (kJ mol^{-1}), standard enthalpy change $\Delta H°$ (kJ mol^{-1}), and standard entropy change $\Delta S°$ (J K^{-1} mol^{-1}). In this study, $\Delta H°$ and $\Delta S°$ were calculated from experimental adsorption data using the Van't Hoff equation as follows:

$$\ln K_d = \frac{\Delta S°}{R} - \frac{\Delta H°}{RT} \tag{13}$$

$$K_d = \frac{q_e}{C_e} \tag{14}$$

where R is the gas constant (8.314 J mol^{-1} K^{-1}), K_d is the distribution coefficient of metal ions between the aqueous phase and the solid phase (L g^{-1}), and T is the absolute temperature (K). The values of $\Delta H°$ and $\Delta S°$ are calculated using the values of the slope ($\Delta H°/R$) and intercept ($\Delta S°/R$) of the linear plot of $\ln K_d$ vs. $1/T$ as shown in Fig. 7. The standard Gibbs free energy change $\Delta G°$ values are calculated according to the following equation:

$$\Delta G° = \Delta H° - T\Delta S° \tag{15}$$

The values of $\Delta G°$, $\Delta H°$, and $\Delta S°$ obtained for Pb^{2+}, Cd^{2+}, and Cr^{3+} ions at 25°C, 35°C, and 45°C are given in Table 4. The values of $\Delta H°$ at 25°C were found to be +10.54, +8.86, and +16.62 kJ mol^{-1} for Cd^{2+}, Pb^{2+}, and Cr^{3+}, respectively. The positive values of $\Delta H°$ indicate the endothermic nature of the adsorption processes of these metal ions on the monolith surface. These results are in agreement with the conclusions drawn from the experiments performed at different temperatures (section 3.1.5 (Effect of temperature)).

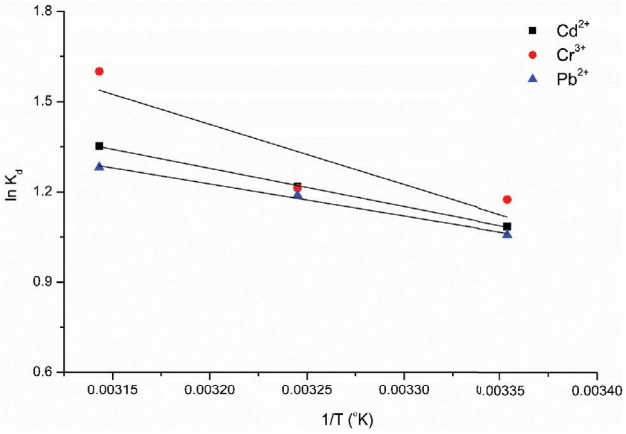

Fig. 7. Plots of $\ln K_d$ vs. $1/T$ for Cd^{2+}, Pb^{2+}, and Cr^{3+} ions at pH = 4.0, temperature = (298–318 K), contact time = 24 h, and monolith dosage = 10 mg/25 mL.

Table 4
Calculated thermodynamic parameters ($\Delta H°$, $\Delta S°$, and $\Delta G°$) for the adsorption of Cd^{2+}, Pb^{2+}, and Cr^{3+} ions onto the polyacrylamide-based monolith at temperature = 298.15, 308.15, and 318.15 K, pH = 4.0, monolith dosage = 10 mg/25 mL, and contact time = 24 h

	$\Delta H°$ (kJ mol^{-1})	$\Delta S°$ (J K^{-1} mol^{-1})	$\Delta G°$ (kJ mol^{-1})		
			298.15 K	308.15 K	318.15 K
Cd^{2+}	10.54	44.4	–2.69	–3.14	–3.59
Pb^{2+}	8.86	38.5	–2.62	–3.00	–3.39
Cr^{3+}	16.62	65.0	–2.76	–3.41	–4.06

Results in Table 4 demonstrate that the adsorption of metal ions on the monolith surface was spontaneous and favorable at the studied temperatures as indicated from the negative values of Gibbs free energy change $\Delta G°$. The positive values of $\Delta S°$ reflect the affinity of the synthesized monolith toward Cd^{2+}, Cr^{3+}, and Pb^{2+} ions. In addition, the positive values of $\Delta S°$ indicate an increase in randomness of adsorption at the solid–liquid interface [20,63].

4. Conclusions

In this work, a macroporous polyacrylamide-based monolith bearing negatively charged interaction sites was synthesized and applied as a new adsorbent for the removal of Cd^{2+}, Pb^{2+}, and Cr^{3+} ions from aqueous solution using batch adsorption technique. The maximum monolayer adsorption capacities for Cd^{2+}, Pb^{2+}, and Cr^{3+} ions are 22.83, 33.33, and 66.67 mg g^{-1}, respectively. The equilibrium data for the metal ions adsorptions were well-fitted to the Langmuir isotherm model. The kinetics of the adsorption processes was found to follow the pseudo-second-order kinetic model. The values of the Freundlich constant (K_F) were increased with increasing the adsorption temperature which confirmed the endothermic nature of Cd^{2+}, Cr^{3+}, and Pb^{2+} adsorption onto the monolith surface. All the adsorption results presented in this study demonstrate that the synthesized monolith can be effectively used for the removal of metal ions from aqueous solutions. In the future, the potential of the synthesized monolith as an adsorbent for the removal of toxic dyes will be explored.

Acknowledgments

Authors thank the University of Jordan (Amman, Jordan) and Al al-Bayt University (Mafraq, Jordan) for providing laboratory facilities and financial support to perform this work.

References

[1] S.P. Dubey, A.D. Dwivedi, M. Sillanpaa, H. Lee, Y.N. Kwon, C. Lee, Adsorption of As(V) by boehmite and alumina of different morphologies prepared under hydrothermal conditions, Chemosphere, 169 (2017) 99–106.
[2] L. Joseph, B.-M. Jun, R.V. Joseph Flora, C.M. Park, Y. Yoon, Removal of heavy metals from water sources in the developing world using low-cost materials: a review, Chemosphere, 229 (2019) 142–159.
[3] N.B. Singh, G. Nagpal, S. Agrawal, Rachna, Water purification by using adsorbents: a review, Environ. Technol. Innovation, 11 (2018) 187–240.
[4] D.D. Mara, Water, sanitation and hygiene for the health of developing nations, Public Health, 117 (2003) 452–456.
[5] A.E. Burakov, E.V. Galunin, I.V. Burakova, A.E. Kucherova, S. Agarwal, A.G. Tkachev, V.K. Gupta, Adsorption of heavy metals on conventional and nanostructured materials for wastewater treatment purposes: a review, Ecotoxicol. Environ. Saf., 148 (2018) 702–712.
[6] M.A. Barakat, New trends in removing heavy metals from industrial wastewater, Arabian J. Chem., 4 (2011) 361–377.
[7] C.K. Ahn, D. Park, S.H. Woo, J.M. Park, Removal of cationic heavy metal from aqueous solution by activated carbon impregnated with anionic surfactants, J. Hazard. Mater., 164 (2009) 1130–1136.
[8] M. Basu, A.K. Guha, L. Ray, Adsorption of lead on cucumber peel, J. Cleaner Prod., 151 (2017) 603–615.
[9] A.A. Al-Massaedh, A. Gharaibeh, S. Radaydeh, I. Al-Momani, Assessment of toxic and essential heavy metals in imported dried fruits sold in the local markets of Jordan, Eur. J. Chem., 9 (2018) 395–400.
[10] K. Belay, Z. Abisa, Developing a method for trace metal analysis in spices using spectroscopic techniques: a review, Int. J. Chem. Nat. Sci., 3 (2015) 195–199.
[11] S. Mahdavi, M. Jalali, A. Afkhami, Heavy metals removal from aqueous solutions using TiO_2, MgO, and Al_2O_3 nanoparticles, Chem. Eng. Commun., 200 (2013) 448–470.
[12] D.M. Chata, A.Y. Iliya, M.S. Chidawa, M.B. Emmanuel, O.O. Juliana, E.K. Chibuzor, Determination of heavy metals in four mango fruit varieties sold in minna modern market, Niger State, Nigeria, Int. J. Biol. Environ. Eng., 1 (2018) 24–29.
[13] A.M. Massadeh, A.A.T. Al-Massaedh, Determination of heavy metals in canned fruits and vegetables sold in Jordan market, Environ. Sci. Pollut. Res., 25 (2018) 1914–1920.
[14] M. Ince, O.K. Ince, An overview of adsorption technique for heavy metal removal from water/wastewater: a critical review, Int. J. Pure Appl. Sci., 3 (2017) 10–19.
[15] G. Zeng, Y. He, Y. Zhan, L. Zhang, Y. Pan, C. Zhang, Z. Yu, Novel polyvinylidene fluoride nanofiltration membrane blended with functionalized halloysite nanotubes for dye and heavy metal ions removal, J. Hazard. Mater., 5 (2016) 60–72.
[16] T. Panayotova, M. Dimova-Todorova, I. Dobrevsky, Purification and reuse of heavy metals containing wastewaters from electroplating plants, Desalination, 206 (2007) 135–140.
[17] B. Renu, M. Agarwal, K. Singh, Methodologies for removal of heavy metal ions from wastewater: an overview, Interdiscip. Environ. Rev., 18 (2017) 124–142.
[18] A.N. Modenes, F.R. Espinoza-Quinones, D.E.G. Trigueros, F.L. Lavarda, A. Colombo, N.D. Mora, Kinetic and equilibrium adsorption of Cu(II) and Cd(II) ions on *Eichhornia crassipes* in single and binary systems, Chem. Eng. J., 168 (2011) 44–51.
[19] F. Fu, Q. Wang, Removal of heavy metal ions from wastewaters: a review, J. Environ. Manage., 92 (2011) 407–418.
[20] M. Alaqarbeh, F.I. Khalili, O. Kanoun, Manganese ferrite ($MnFe_2O_4$) as potential nanosorbent for adsorption of uranium(VI) and thorium(IV), J. Radioanal. Nucl. Chem., 323 (2020) 515–537.
[21] O. Hamdaoui, E. Naffrechoux, Modeling of adsorption isotherms of phenol and chlorophenols onto granular activated carbon Part I. Two-parameter models and equations allowing determination of thermodynamic parameters, J. Hazard. Mater., 147 (2007) 381–394.

[22] N. Ouasfi, M. Zbair, E. Sabbar, L. Khamliche, High performance of Zn–Al–CO_3 layered double hydroxide for anionic reactive blue 21 dye adsorption: kinetic, equilibrium, and thermodynamic studies, Nanotechnol. Environ. Eng., 4 (2019) 1–13, doi: 10.1007/s41204-019-0063-5.
[23] G. Sharma, D. Pathania, M. Naushad, N.C. Kothiyal, Fabrication, characterization and antimicrobial activity of polyaniline Th(IV) tungstomolybdophosphate nanocomposite material: efficient removal of toxic metal ions from water, Chem. Eng. J., 251 (2014) 413–421.
[24] J.A. Kumar, D.J. Amarnath, G. Narendrakumar, K.V. Anand, Optimization of process parameters for naphthalene removal onto nano.iron oxide/carbon composite by response surface methodology, isotherm and kinetic studies, Nanotechnol. Environ. Eng., 3 (2018) 1–12, doi: 10.1007/s41204-018-0046-y.
[25] G. Sharma, M. Naushad, Adsorptive removal of noxious cadmium ions from aqueous medium using activated carbon/zirconium oxide composite: isotherm and kinetic modelling, J. Mol. Liq., 310 (2020) 113025, doi: 10.1016/j.molliq.2020.113025.
[26] G. Sharma, M. Naushad, D. Pathania, A. Mittal, G.E. El-desoky, Modification of *Hibiscus cannabinus* fiber by graft copolymerization: application for dye removal, Desal. Water Treat., 54 (2015) 3114–3121.
[27] K.B. Payne, T.M. Abdel-Fattah, Adsorption of divalent lead ions by zeolites and activated carbon: effects of pH, temperature, and ionic strength, J. Environ. Sci. Health, Part A, 39 (2005) 2275–2291.
[28] G. Limousin, J.-P. Gaudet, L. Charlet, S. Szenknect, V. Barthes, M. Krimissa, Sorption isotherms: a review on physical bases, modeling and measurement, Appl. Geochem., 22 (2007) 249–275.
[29] M. Sharma, J. Singh, S. Hazra, S. Basu, Remediation of heavy metal ions using hierarchically porous carbon monolith synthesized via nanocasting method, J. Environ. Chem. Eng., 6 (2018) 2829–2836.
[30] Y.S. Al-Degs, M.I. El-Barghouthi, A.H. El-Sheikh, G.M. Walker, Effect of solution pH, ionic strength, and temperature on adsorption behavior of reactive dyes on activated carbon, Dyes Pigm., 77 (2008)16–23.
[31] A. Ali, A. Mannan, l. Hussain, I. Hussain, M. Zia, Effective removal of metal ions from aqueous solution by silver and zinc nanoparticles functionalized cellulose: isotherm, kinetics and statistical supposition of process, Environ. Nanotechnol. Monit. Manage., 9 (2018) 1–11.
[32] M.A. Zaitoun, M.A. Al-Anber, I.F. Al Momani, Sorption and removal of aqueous iron(III) ion by tris (2-aminoethyl)amine moiety functionalized silica gel, Int. J. Environ. Anal. Chem., 100 (2020) 1446–1467.
[33] S.T. Ramesh, N. Rameshbabu, R. Gandhimathi, P.V. Nidheesh, M. Srikanth Kumar, Kinetics and equilibrium studies for the removal of heavy metals in both single and binary systems using hydroxyapatite, Appl. Water Sci., 2 (2012) 187–197.
[34] P. Chassary, T. Vincent, E. Guibal, Metal anion sorption on chitosan and derivative materials: a strategy for polymer modification and optimum use, React. Funct. Polym., 60 (2004)137–149.
[35] F.I. Khalili, N.H. Salameh, M.M. Shaybe, Sorption of Uranium(VI) and Thorium(IV) by Jordanian Bentonite, J. Chem., 2013 (2013) 1–13.
[36] F. Al-rimawi, M. Daana, M. Khamis, R. Karaman, H. Khoury, M. Qurie, Removal of selected pharmaceuticals from aqueous solutions using natural Jordanian zeolite, Arabian J. Sci. Eng., 44 (2019) 209–215.
[37] R.I. Yousef, B. El-Eswed, M. Alshaaer, F. Khalili, H. Khoury, The influence of using Jordanian natural zeolite on the adsorption, physical, and mechanical properties of geopolymers products, J. Hazard. Mater., 165 (2009) 379–387.
[38] Y. Zhang, Y. Li, Y. Ning, D. Liu, P. Tang, Z. Yang, Y. Lu, X. Wang, Adsorption and desorption of uranium(VI) onto humic acids derived from uranium-enriched lignites, Water Sci. Technol., 77 (2018) 920–930.
[39] M. Sharma, D. Choudhury, S. Hazra, S. Basu, Effective removal of metal ions from aqueous solution by mesoporous MnO_2 and TiO_2 monoliths: kinetic and equilibrium modelling, J. Alloys Compd., 720 (2017) 221–229.
[40] M. Sharma, S. Hazra, S. Basu, Kinetic and isotherm studies on adsorption of toxic pollutants using porous ZnO@SiO_2 monolith, J. Colloid Interface Sci., 504 (2017) 669–679.
[41] R.J. Groarke, D. Brabazon, Methacrylate polymer monoliths for separation applications, Materials, 9 (2016) 446–479.
[42] I. Nisschang, T.J. Causon, Porous polymer monoliths: from their fundamental structure to analytical engineering applications, TrAC, Trends Anal. Chem., 75 (2016) 108–117.
[43] S. Xie, F. Svec, J.M.J. Frechet, Porous polymer monoliths: preparation of sorbent materials with high-surface areas and controlled surface chemistry for high-throughput, online, solid-phase extraction of polar organic compounds, Chem. Mater., 10 (1998) 4072–4078.
[44] A.A. Al-Massaedh, M. Schmidt, U. Pyell, U.M. Reinscheid, Elucidation of the enantiodiscrimination properties of a nonracemic chiral alignment medium through gel-based capillary electrochromatography: separation of the mefloquine stereoisomers, ChemistryOpen, 5 (2016) 455–459.
[45] A.A. Al-Massaedh, U. Pyell, Mixed-mode acrylamide-based continuous beds bearing *tert*-butyl groups for capillary electrochromatography synthesized via complexation of *N-tert*-butylacrylamide with a water-soluble cyclodextrin. Part I: retention properties, J. Chromatogr. A, 1477 (2016) 114–126.
[46] L. Uzun, D. Turkmen, E. Yilmaz, S. Bektas, A. Denizli, Cysteine functionalized poly(hydroxyethyl methacrylate) monolith for heavy metal removal, Colloids Surf., A, 330 (2008) 161–167.
[47] S. Wang, R. Zhang, Column preconcentration of lead in aqueous solution with macroporous epoxy resin-based polymer monolithic matrix, Anal. Chim. Acta, 575 (2006) 166–171.
[48] S.K.A. Rahman, N.A. Yusof, F. Mohammad, A.H. Abdullah, A. Idris, Ion imprinted polymer monoliths as adsorbent materials for the removal of Hg(II) from real-time aqueous samples, Curr. Sci., 113 (2017) 2282–2291.
[49] G. Guiochon, Monolithic columns in high-performance liquid chromatography, J. Chromatogr. A, 1168 (2007) 101–168.
[50] A.A. Al-Massaedh, U. Pyell, Adamantyl-group containing mixed-mode acrylamide-based continuous beds for capillary electrochromatography. Part IV: investigation of the chromatographic efficiency dependent on the retention mode, J. Chromatogr. A, 1349 (2014) 80–89.
[51] A.A. Al-Massaedh, F.I. Khalili, Removal of thorium(IV) ions from aqueous solution by polyacrylamide-based monoliths: equilibrium, kinetic and thermodynamic studies, J. Radioanal. Nucl. Chem., 327 (2021) 1201–1217.
[52] S.I.Y. Salameh, F.I. Khalili, A.H. Al-Dujaili, Removal of U(VI) and Th(IV) from aqueous solutions by organically modified diatomaceous earth: evaluation of equilibrium, kinetic and thermodynamic data, Int. J. Miner. Process., 168 (2017) 9–18.
[53] Y. Zhu, W. Wang, Y. Zheng, F. Wang, A. Wang, Rapid enrichment of rare-earth metals by carboxymethyl cellulose-based open-cellular hydrogel adsorbent from HIPEs template, Carbohydr. Polym., 140 (2016) 51–58.
[54] E. Igberase, P. Osifo, A. Ofomaja, The adsorption of Pb, Zn, Cu, Ni, and Cd by modified ligand in a single component aqueous solution: equilibrium, kinetic, thermodynamic, and desorption studies, Int. J. Anal. Chem., 2017 (2017) 1–15, doi: 10.1155/2017/6150209.
[55] J. Aguado, J.M. Arsuaga, A. Arencibia, M. Lindo, V. Gascon, Aqueous heavy metals removal by adsorption on amine-functionalized mesoporous silica, J. Hazard. Mater., 163 (2009) 213–221.
[56] Y.S. Ho, G. McKay, Pseudo-second order model for sorption processes, Process Biochem., 34 (1999) 451–465.
[57] D. Robati, Pseudo-second-order kinetic equations for modeling adsorption systems for removal of lead ions using multi-walled carbon nanotube, J. Nanostruct. Chem., 3 (2013)1–6.
[58] C.H. Giles, D. Smith, A general treatment and classification of the solute adsorption isotherm, J. Colloid Interface Sci., 47 (1974) 755–765.
[59] S. Liu, Cooperative adsorption on solid surfaces, J. Colloid Interface Sci., 450 (2015) 224–238.

[60] W.F. Jaynes, S.A. Boyd, Hydrophobicity of siloxane surfaces in smectites as revealed by aromatic hydrocarbon adsorption from water, Clays Clay Miner., 39 (1991) 428–436.
[61] U.F. Alkaram, A.A. Mukhlis, A.H. Al-Dujaili, The removal of phenol from aqueous solutions by adsorption using surfactant-modified bentonite and kaolinite, J. Hazard. Mater., 169 (2009) 324–332.
[62] D. Xu, X.L. Tan, C.L. Chen, X.K. Wang, Adsorption of Pb(II) from aqueous solution to MX-80 bentonite: effect of pH, ionic strength, foreign ions and temperature, Appl. Clay Sci., 41 (2008) 37–46.
[63] Y. Hu, S. Giret, R. Meinusch, J. Han, F.-G. Fontaine, F. Kleitz, D. Lariviere, Selective separation and preconcentration of Th(IV) using organo-functionalized, hierarchically porous silica monoliths, J. Mater. Chem. A, 7 (2019) 289–302.